IEEE Access
Multidisciplinary ⋮ Rapid Review ⋮ Open Access Journal

Received January 13, 2021, accepted January 30, 2021, date of publication February 3, 2021, date of current version March 25, 2021.

Digital Object Identifier 10.1109/ACCESS.2021.3056774

Improved High-Performance Solution Processed In_2O_3 Thin Film Transistor Fabricated by Femtosecond Laser Pre-Annealing Process

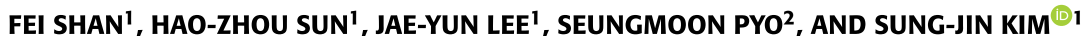

FEI SHAN[1], HAO-ZHOU SUN[1], JAE-YUN LEE[1], SEUNGMOON PYO[2], AND SUNG-JIN KIM[1]

[1]College of Electrical and Computer Engineering, Chungbuk National University, Cheongju 28644, South Korea
[2]Department of Chemistry, Konkuk University, Seoul 05029, South Korea

Corresponding author: Sung-Jin Kim (ksj@cbnu.ac.kr)

This research was supported by the MSIT (Ministry of Science and ICT), Korea, under the Grand Information Technology Research Center support program (Grant No. IITP-2020-0-01462) supervised by the IITP (Institute for Information and Communications Technology Planning and Evaluation), and by the Basic Science Research Program through the National Research Foundation of Korea (NRF) funded by the Ministry of Education (Grant No.2020R1I1A3A04037800). This research was also supported by Basic Science Research Program through the National Research Foundation of Korea (NRF) funded by the Ministry of Education (No. 2020R1A6A1A1204794511).

ABSTRACT The low-temperature annealing process has a critical impact on the electrical performance of thin-film transistors (TFTs). This paper reports significant performance enhancements of TFTs using a femtosecond laser pre-annealing (FLA)-based preparation method. The solution-processed In_2O_3 films were fabricated by FLA at various laser irradiation times and then annealed on a hot-plate at 230 °C. When the FLA time was set to 30 s, the device exhibited high saturation mobility of 10.03 ± 0.64 cm^2/Vs, I_{on}/I_{off} of 3.4 × 10^5, low V_{TH} of 0.14 ± 0.64 V, and small SS of 1.44 ± 0.37 V/dec. The FLA process improved the formation of M-O lattices effectively, which led to an improvement in mobility. Furthermore, the gate-bias-stress stability and time-dependent environmental stability were improved considerably by the FLA process. These results show that high-performance In_2O_3 TFTs can be prepared at low temperatures using FLA-centered annealing technology. This work suggests that the FLA preparation method has tremendous potential for the fabrication of low-cost, high performance, and flexible TFT devices.

INDEX TERMS In_2O_3, thin-film transistors, solution process, femtosecond laser, low-temperature, annealing process.

I. INTRODUCTION

Over the past decade, amorphous metal oxide semiconductors (AMOS) [1]–[3] have been studied widely as channel materials for thin-film transistors (TFTs) [4] in active-matrix displays [5], [6], biochemical sensors [7], logic circuits [8], and flexible displays owing to their superior effective electron mobility, high transparency (> 80 %) in the visible region, good atmospheric stability, excellent uniformity compared to polysilicon TFTs, and low-temperature processing [1], [2] Recently, research into TFTs based on metal oxide materials has focused mainly on amorphous binary, ternary and quaternary metal oxide materials, such as indium zinc oxide (IZO) [9], indium gallium zinc oxide (IGZO) [10], [11], zinc tin oxide (ZTO) [12], [13], indium zinc tin oxide (IZTO) [14], and indium oxide (In_2O_3). These materials can also be used as solution-processable materials for oxide-based TFTs that can provide a viable route for low-cost TFT applications. In particular, the binary In_2O_3 has tremendous potential in various applications that because of its excellent electron conductivity [15], [16], single-crystal mobility of up to 160 $cm^2V^{-1}s^{-1}$ grown from the vapor-phase at 1000 °C [17], high optical transparency [18] in the visible range (> 90%) given by its wide bandgap between 3.6 and 3.75 eV [19], [20], and large-area uniformity [21].

In_2O_3-based TFTs are popular for high-resolution active-matrix displays owing to its solution processing, which offers a scalable and cost-effective route for low-cost, equipment simplicity, high throughput, low material waste, and large-area deposition [3], [22], [23] compared to other deposition techniques, such as evaporation [24], sputtering [25], chemical vapor deposition [19], [26], and atomic layer deposition [27], [28]. In addition, the preparation of In_2O_3 thin films is entirely independent of

The associate editor coordinating the review of this manuscript and approving it for publication was Sun Junwei.

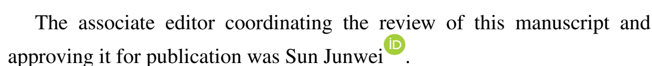

This work is licensed under a Creative Commons Attribution 4.0 License. For more information, see https://creativecommons.org/licenses/by/4.0/

2-methoxyethanol/acetonitrile-based liquid precursor solutions. Therefore, high-temperature annealing processing, which aims to remove volatile organics and achieve full oxide lattice condensation, is not an essential step, which would result in less damage to the environment[29] Simple solution processing also avoids the retention of organic residues following the subsequent low-temperature annealing process, which affects the metal thin film formation and the electrical performance of TFTs devices [30], [31] Most studies of solution-processed TFTs have shown that a high-temperature annealing process is essential for excellent electrical performance. On the other hand, in terms of the low-temperature annealing process, the field-effect electron mobility of solution-processed In_2O_3 TFTs shows large fluctuations with mobilities of 0.29 $\sim$ 24.85 $cm^2V^{-1}s^{-1}$ [32] and 0.85 $\sim$ 22.14 $cm^2V^{-1}s^{-1}$ [33] at temperatures ranging from 200 to 300 °C. In particular, a poor mobility less than 1 $cm^2V^{-1}s^{-1}$ has been observed at a low-temperature of 200 °C. Therefore, further study of low-temperature annealing technology ($\leq$ 250 °C) is necessary, while ensuring excellent electrical performance [34]–[36] Furthermore, it will promote the use of flexible substrates for device fabrication, such as low-cost plastic substrates.

Many low-temperature annealing techniques have been used for the preparation of In_2O_3 thin films, including sol-gel on-chip processes [37], deep-ultraviolet photochemical activation [38], combustion processes [39], ozone photo-annealing [21], high-pressure annealing [40], microwave-assisted annealing [33], aqueous route [41], and laser annealing. In particular, many laser annealing methods have been used to manufacture metal oxide films with their economic and ecological advantages. On the other hand, few studies have explored In_2O_3 films fabricated by femtosecond laser-assisted annealing. Femtosecond laser annealing (FLA) technology seldom needs to be used in a high-pressure vacuum environment. In addition, it is not a time-consuming process because of its ultrashort laser pulse and high transient intensity, resulting in lower energy cost and less damage to the metal oxide thin film [42] The high-energy efficiency femtosecond laser is also more suitable for the low-temperature annealing process of In_2O_3 films than other candidate technologies. This is because the preparation of an In_2O_3 solution does not require a 2-methoxyethanol/acetonitrile-based precursor. Hence, high-temperature annealing to decompose the precursor is not needed. An optimized In_2O_3 film preparation process by femtosecond laser would be needed to achieve the potential advantages and overcome the challenges associated with the application of FLA to improve the poor electrical characteristics (especially mobility) of In_2O_3 TFTs after low annealing temperatures.

This paper reports a novel annealing approach using a femtosecond laser pre-annealing-based multiple annealing process at 230 °C to prepare solution-processed In_2O_3 TFTs with enhanced electrical performance. This unique annealing process, including fast femtosecond laser pre-annealing and low-temperature annealing at 230 °C under ambient conditions, offers a simple, low-cost, and pro-environmental preparation method. The effects of this approach on the optical, morphological, chemical, and electrical properties were examined by tuning the irradiation time of the femtosecond laser. In addition, the influence of the femtosecond laser pre-annealing on In_2O_3 TFTs was examined by comparison with a non-irradiated one. The improved high-performance solution-processed In_2O_3 TFTs provide an original and effective annealing method that would be suitable for flexible substrates as well as viable low-cost preparation.

II. EXPERIMENTAL DETAILS

An indium nitrate hydrate [$In(NO_3)_3 \cdot xH_2O$] with a purity of 99.99% was dissolved in pure water (ACS reagent) to yield a 0.1 M In_2O_3 solution. All reagents were purchased from ALDRICH and used as received. An In_2O_3 solution was stirred for 2 h at 45 °C by a magnetic stirrer at 700 rpm. The prepared clear solution was then filtered through a 0.20 μm syringe filter before spin coating to obtain a more transparent homogeneous solution.

A bottom-gate and top-contact source-drain electrode structure was used to fabricate In_2O_3 TFTs, as shown in Figure 1(a), the substrate consisted of a 100 nm thick SiO_2 layer on a heavily doped n-type silicon wafer (thickness of 710-740 μm) as the gate dielectric layer. The SiO_2/Si wafer was rinsed with a water-dissolved powder detergent and sonicated sequentially in deionized water, acetone, and isopropyl alcohol at 45 °C for 15 min, and blow-dried with N_2 gas. Subsequently, the samples were dried in an oven at 45 °C for 30 min to remove all residual solvent. SiO_2/Si wafers were then placed in an ultraviolet treatment cleaner at 28 mW for 20 min to form a hydrophilic surface in the channel area.

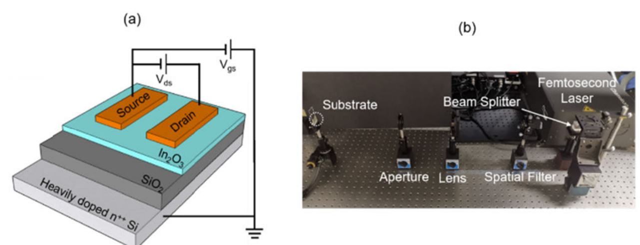

FIGURE 1. Schematic diagram of (a) the In_2O_3 TFT structure, and (b) the experiment setup for femtosecond laser pre-annealing.

The prepared In_2O_3 solution, which had been filtered through a 0.20 μm syringe filter, was spin-coated at 3000 rpm for 30 s. The resulting coated substrate was then soft-baked on a hot-plate (AS ONE, HPR6-1515) at 80 °C for 5 min in air. After cooling, the In_2O_3 thin films were pre-annealed by a femtosecond laser for various treatment time (30, 60, and 90 s) at a wavelength of 700 nm. The femtosecond laser was generated using a chameleon Ti: sapphire lasers system (COHERENT, USA). Figure 1(b) shows the laser annealing setting. The In_2O_3 thin film-based wafer was mounted on the left holder. The input laser beam (laser power of 1860 mW) was converted to an output laser beam using a beam splitter.

A spatial filter was used to ensure the output laser operated at a lower-order mixed-mode and improve the beam quality. Finally, the high-quality output laser beam was focused on the surface of the In_2O_3 film using a lens at a point power of 97 W/cm^2, and the beam was adjusted to cover the square wafer completely using an aperture. Femtosecond laser pre-annealing, through which optical energy was transferred to the In_2O_3 films, produced a large number of electrons, and the energy was transferred to the lattice. The laser pre-annealing process was operated with constant humidity and operating temperature range of 15 to 28 °C in a dark room in air. The pre-annealed substrates were annealed on a hot-plate at 230 °C for 2 h in air. In the end, the Al source/drain electrodes were deposited onto the In_2O_3 layer by thermal evaporation (pressure $\sim 10^{-6}$ Torr, a rate of 0.1 Å/s) using a shadow mask, which resulted in a channel area, 200 μm in length and 2000 μm in width.

The electrical characteristics, including the output, transfer, stability, and negative-bias-stress (NBS)/positive-bias-stress (PBS) curves, were measured using a semiconductor parameter analyzer (Keithley 4200, Keithley Instruments LLC, Cleveland, Ohio) in a vacuum glovebox workstation (MBRAUN MB-Labstar Pro SP, filled with nitrogen) under ambient conditions in a dark room. The surface morphologies of the In_2O_3 films were characterized by atomic force microscopy (AFM, ICON, Bruker Corporation). The chemical structures of In_2O_3 thin films were investigated by X-ray photoelectron spectroscopy (XPS, Quantera-II, Physical Electronics, Inc. Chanhassen, MN, USA) on actual In_2O_3 TFTs devices prepared without an Al electrode. X-ray beams (100 μm at 25 W and 15 kV) were used to radiate a surface measurement range of 1000 $\times$ 1000 μm.

III. RESULTS AND DISCUSSION

The bottom-gate and top-contact TFTs were fabricated on SiO_2 substrates coated with In_2O_3 channel films by FLA at three different radiation times (30, 60, and 90 s) followed by low-temperature annealing processing (annealing temperature of 230 °C). Figure 1(a) presents the TFT structure. FLA processing showed an integration interaction between high-energy photons and the In_2O_3 channel films, in which the optical energy is transferred to the surface of the material to generate a large number of electrons. These electrons transfer energy to the lattice, which modifies the material phase or structure in the irradiated area. During the energy transfer process through nonlinear ionization, the laser pulse width is greater than 10 fs, which is shorter than the electron-phonon scattering time over a picosecond timescale. This leads to the excitation of bound electrons by the high transient intensity laser under lower energy [43], [44] An applied electric field is formed through a charge separation process with the escaped electrons, and the conduction of mobile electrons under this electric field is closely related to the improvement in TFT performance.

The FLA-centered low-temperature annealing process was used to improve the electrical performance of the TFTs device to replace traditional thermal annealing. For comparison, control In_2O_3-based TFTs were fabricated by single annealing processing on a hot-plate at 230 °C. The electrical characteristics of the In_2O_3 TFTs treated with single thermal annealing and the FLA-centered annealing process with different laser radiation times (30, 60, and 90 s) were carried out in a dark ambient environment by measuring the output and transfer characteristic curves as a function of the drain and back gate voltages. Figure 2 shows the summarized output curves of the In_2O_3 TFTs at gate voltage (V_{GS}) from 0 to 30 V. The device without the FLA process exhibited typical n-channel behavior with clear current saturation and pinch-off voltage, as shown in Figure 2(a). Figure 2(b-d) presents the fluctuating output curves of the devices fabricated using the FLA process. The In_2O_3 TFTs with a 30 s FLA process exhibited the best contact, solid saturation, and clearer pinch-off that was even better than the sample device without FLA. In contrast, the output characteristics deteriorated when the laser radiation time was more than 60 s.

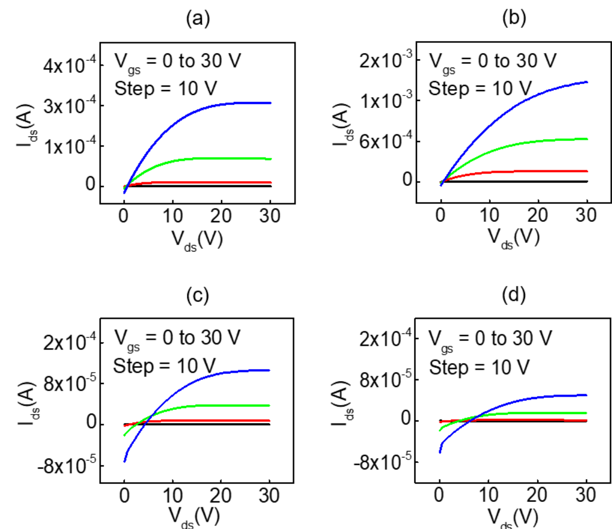

FIGURE 2. Output curves of (a) In_2O_3 TFT by single thermal annealing at 230 °C and In_2O_3 TFTs using the FLA process at (b) 30, (c) 60, and (d) 90 s.

Figure 3 shows the transfer characteristic curves, which were obtained by measuring the drain current (I_{DS}) as a function of V_{GS} from 0 to 30 V at a fixed drain voltage (V_{DS}) of 30 V. Both devices exhibited typical n-type characteristics. Hence, the I_{DS} increased to various extents with increasing laser time. The most significant change in I_{DS} was observed at 30 s (Figure 3(b)). The threshold voltage (V_{TH}) shifted to the negative gate bias direction with increasing FLA processing time. The charge carrier mobility in the saturation region (μ_{sat}) was calculated from the following equation according to the conventional TFTs model:

$$\mu_{sat} = \frac{2L}{WC_i}\left(\frac{\partial\sqrt{I_{DS}}}{\partial V_{GS}}\right)^2 \quad (1)$$

where C_i is the areal capacitance of the gate dielectric, and W and L are the channel width and length, respectively.

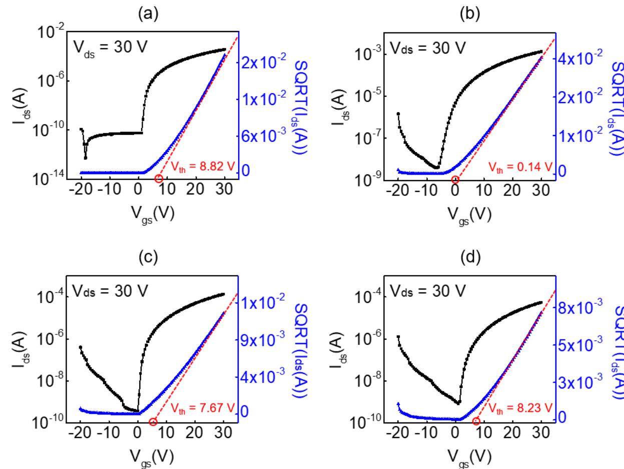

FIGURE 3. Transfer curves with SQRT (right-axis) curves of solution-processed In_2O_3 TFTs obtained under different annealing conditions: (a) by single thermal annealing at 230 °C, using the FLA process at (b) 30, (c) 60, and (d) 90 s. The measurements were performed at the saturation region with $V_{DS} = 30$ V.

Table 1 lists the electrical characteristics with different laser radiation times compared to the device without the FLA process. The device with a single annealing process at 230 °C exhibited normal performance, including a low μ_{sat} of 3.92 ± 0.18 cm^2/Vs, a high on/off current ratio (I_{on}/I_{off}) of 8.4 × 10^6, a high V_{TH} of 8.82 ± 0.50 V, and a small subthreshold swing (SS) of 0.78 ± 0.13 V/dec, which is similar to previous reports [32], [33] The device performance was strongly dependent on the laser radiation time. The μ_{sat} values of the In_2O_3 TFTs with the FLA process at 30, 60, and 90 s were calculated to be 10.03 ± 0.64, 1.12 ± 0.20, and 0.72 ± 0.03 cm^2/Vs, respectively. Correspondingly, the I_{on}/I_{off} values decreased from 3.4 × 10^5 and 3.7 × 10^5 to 6.8 × 10^4 with increasing laser radiation time. All SS values of the In_2O_3 TFTs devices showed slight fluctuations around 0-1 V/dec. Although the TFTs device fabricated with the FLA process for 30 s showed a slightly lower I_{on}/I_{off} value of 3.4 × 10^5, it exhibited the highest μ_{sat} of 10.03 ± 0.64 cm^2/Vs and a significantly lower V_{TH} of 0.14 ± 0.64 V. Although the TFTs device fabricated with the FLA process for 30 s showed a slightly lower Ion/Ioff value of 3.4 × 10^5, it exhibited the highest μsat of 10.03 ± 0.64 cm^2/Vs and a significantly lower V_{TH} of 0.14 ± 0.64 V. On the other hand, the field-effect electron mobility of solution-processed In_2O_3 TFTs with PLA and low-temperature preparation process of 230 °C shows good improvement compared with reported research. Especially, under the similar temperature range from 200 to 250 °C, the highest μsat of 10.03 ± 0.64 cm^2/Vs and the lower V_{TH} of 0.14 ± 0.64 V of our solution processed oxide TFT better than most solution processed oxide TFTs in low-temperature preparation areas (mobility < 9 cm^2/Vs) [45]–[47] In particular, a poor mobility less than 1 cm^2/Vs has been observed at a low-temperature of 200 °C. These values were superior to the single annealed device and the FLA process-fabricated devices at other laser radiation times. The device exhibited similar μ_{sat} values reported to date for In_2O_3 TFTs prepared from solution and annealed at the same low-temperature of 230 °C.

TABLE 1. Electrical properties of solution-processed In_2O_3 TFTs at various FLA times.

Femtosecond laser irradiation time (s)	μ_{sat} (cm^2/Vs)	I_{on}/I_{off}	V_{th} (V)	S/S (V/dec)
0	3.92 ± 0.18	8.4 × 10^6	8.82 ± 0.50	0.78 ± 0.13
30	10.03 ± 0.64	3.4 × 10^5	0.14 ± 0.64	1.44 ± 0.37
60	1.12 ± 0.20	3.7 × 10^5	7.67 ± 1.09	0.84 ± 0.16
90	0.72 ± 0.03	6.8 × 10^4	8.23 ± 0.71	1.09 ± 0.06

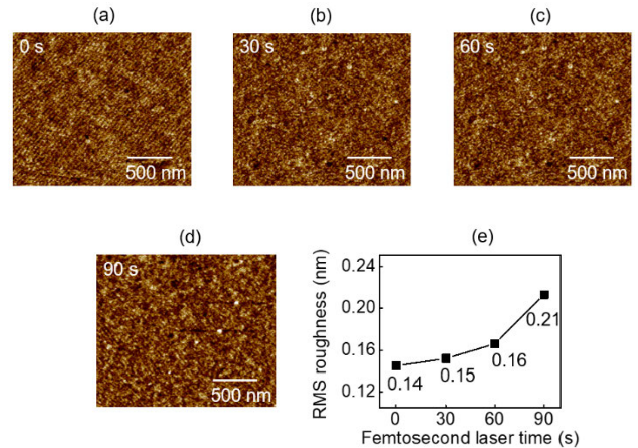

FIGURE 4. AFM images of In_2O_3 films fabricated by (a) low-temperature annealing or FLA processes at (b) 30, (c) 60, and (d) 90 s. (e) R_{RMS} values summarization of these In_2O_3 films.

Figure 4 presents atomic force microscopy (AFM) images of In_2O_3 films and the resulting film qualities through the root-mean-square roughness (R_{RMS}). The In_2O_3 film grown at 230 °C was quite smooth and uniform, and the grain structure was almost non-existent on the surface owing to its amorphous state, as shown in Figure 4(a). Interestingly, Figures 4(b-d) show a particular change in the state of In_2O_3 films fabricated by the FLA process at various laser radiation times (30, 60, and 90 s) in that the surfaces exhibit a systematic and small increase in the grains over laser time. The R_{RMS} values of the In_2O_3 films were measured to be 0.14, 0.15, 0.16, and 0.21 nm, as shown in Figure 4(e). The interface roughness of the channel layers is also an important factor for the performance of TFTs because a smooth interface could improve charge-carrier transportation and reduce physical traps. The results of R_{RMS} showed no significant difference, even though the crystallinity changes with increasing laser radiation time, and is accompanied only by a slightly increased R_{RMS} value of 0.07 nm. All the In_2O_3 films, including the film with a single low-temperature and the films with the FLA process, showed smooth surfaces and high-quality $R_{RMS} < 0.22$ nm. The FLA process could increase the density

of oxygen vacancies (O_V) inside the In_2O_3 films because the oxygen inside the films is dissociated and diffused by the high-energy efficient femtosecond laser. Native defect doping occurs via the formation of double-charged oxygen vacancies (V_O^{2+}) based on related studies about crystalline In_2O_3, [48] which can be expressed by the equilibrium reaction:

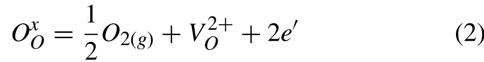

$$O_O^x = \frac{1}{2}O_{2(g)} + V_O^{2+} + 2e' \quad (2)$$

where the formation of an O_V on the oxygen sublattice, O_O^x, liberates two electrons. FLA and low-temperature annealing processes in an ambient environment could induce crystallization and reduce O_V. Therefore, the increase in laser radiation time results in a gradual increase in the R_{RMS} values.

Although the laser annealed In_2O_3 TFTs for 30 s showed an excellent mobility, the laser annealed In_2O_3 TFTs for 60 and 90 s exhibited drastically decreased field effect characteristics. Therefore, a possible thermal damage in FLA process is how to explain the key performance degradation issues compared with 30 s annealed sample. Typically, laser annealing for a short time the influence of femtosecond laser on the oxide thin film is negligible and certainly do not cause extreme thermal damage to oxide film with sufficient buffer oxide thickness due to its short wavelength and extremely short pulse. But in this work, the irradiation of the femtosecond laser with high energy density (a point power of 97 W/cm^2) and wavelength of 700 nm onto a locally confined area of In2O3 film, the temperature of the film surface (In_2O_3 film thickness < 10 nm) instantaneously reaches thousands of kelvins. The active channel layer will be affected by thermal annealing effect without thermal damage induced by heat diffusion that assumes the FLA process is short enough. To avoid that, the laser irradiation time should be carefully optimized. The continued deterioration of R_{RMS} data with the change of laser irradiation time also illustrate this point.

It seems that the interfacial roughness changes slightly based on R_{RMS} not only is an important theoretical basis, but interface traps may also cause carrier scattering and trapping to various extents. In addition, the differences in TFTs performance by various laser irradiation time could be attributed in some way to the different defect density of the insulator/semiconductor interface. The interface trap densities (N_T) at the channel/dielectric interfaces were calculated by the following equation and related to the SS values from the transfer curves [49]:

$$N_T = \frac{C_i}{q}\left[\frac{SS\log(e)}{{}^{kT}/_{q}} - 1\right] \quad (3)$$

where k is Boltzmann's constant, e is the base of natural logarithm, T is the temperature, and q is the electron charge. It shows that the interface trap density is germane to SS, and the positive shift in V_{TH} from 30 to 90 s accompanying the change of SS caused by charge trapping and creation of defects.

The changes in the oxygen-related form have a strong tie with the electrical performance of the TFT device. The effects of the FLA process at various laser radiation times on the In_2O_3 TFTs were investigated by measuring the stoichiometry of the In_2O_3 films by XPS. Figure 5(a-d) shows the XPS spectra of the single low-temperature annealing and FLA-centered annealing fabricated films. The O 1s core spectrum of In_2O_3 was deconvoluted into three peaks centered at 529.8 (O_1), 531.2 (O_2), and 532.4 (O_3) eV, which were assigned to the oxygen in metal-oxide lattices (M-O lattices), O_V, and hydroxide-related species (OH species), respectively. The variation in the peak ratio of the M-O lattices and O_V confirmed that all the In_2O_3 films had an amorphous structure because the In_2O_3 film with a crystalline structure should show the highest peak of the M-O lattice and lower O_V peak [50] Figure 5(e) shows the area in the O1 peak analysis based on the M-O lattices and O_V state. The intensity of the M-O lattices and peak ratio the intensity of O_V increased with increasing FLA laser radiation time. When the laser treatment time was 30 s, the relative quantity of M-O lattices increased from 27.1% to 31.7%, and that of O_V decreased from 44.1% to 38.7% compared to the sample In_2O_3 film produced using the simple annealing process. The O 1s results indicate that the low-temperature annealing technology, which was improved by the femtosecond laser in the annealing preparation processes, could promote the formation of the M-O lattices and prevent the production of the O_V. The increase in the number of M-O lattices can improve the electron transport channel and facilitate efficient charge transport through the vacant $4d^{10}5s^0$ s-state metal cations. The s-states overlapped with each other because of the huge spatial expanse of the vacant s-states, facilitating electron transport and resulting in increased mobility [51], [52] The formation of M-O lattices plays a vital role in improving the carrier transport. The FLA process at 30 s could form more M-O lattices and then improve the μ_{sat} value to 10.03 ± 0.64 cm^2/Vs, which is consistent with Table 1. After longer laser irradiation (60 and 90 s), the intensity of M-O lattices is observed to decreased, which present the formation of oxygen deficiency state, resulting in the reduction in carrier density. Charge transport in the channel layer is affected by percolation conduction, [9] which means the O_V can convert to trap states and hinder charge transport. Therefore, the FLA process at 30 s could also restrain the production of O_V as low as 38.7%, further improving the mobility, and simultaneously leading the negative shift in V_{TH}, as shown in Figure 3(b). Instead, the positive shift in V_{TH} with the increase in laser irradiation time, which is also able to extrapolate from the slop of the drain current increase, resulted in apparent reduction in source-to-drain current.

On the other hand, the relative quantity of M-O lattices decreased continuously with increasing FLA irradiation time (30, 60, and 90s) from 31.7% to 25.7%, even below 27.1% for the In_2O_3film. The O_V increased from 38.7% to 43.7%. The femtosecond laser irradiation, to a certain extent, played a photo-assisted role in removing the OH-related species and

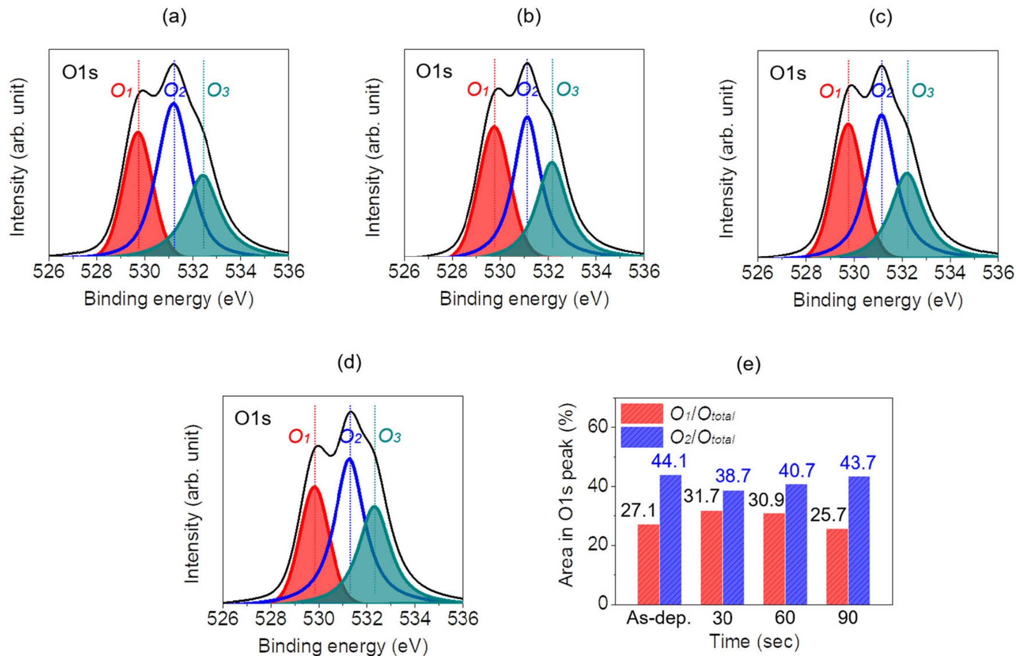

FIGURE 5. XPS O 1s analysis of In_2O_3 films annealed using (a) low-temperature annealing or FLA processes at (b) 30, (c) 60, and (d) 90 s. (3) The area in O1 peak analysis based on the M-O lattices and O_V states increases with increasing laser irradiation time.

residual impurity deteriorate the device performance because of its high energy photons [11], [53] Unfortunately, the fraction of OH species appeared to fluctuate slightly. Moreover, the effects of the FLA were not evident, also meaning the incomplete formation of the M-O lattices. In addition to the limit of the FLA process operated at a low laser power of 1.86 W, thermal annealing was performed in the subsequent preparation process, which led to inconspicuous photo-assisted effects. A proper FLA time can decrease the crystal lattice distortion, but the I_{on}/I_{off} values of the TFT devices decreased by approximately 10^2 with increasing laser-irradiation time. The M-O lattices are unable to recover adequately, and the growing V_O^{2+} augment the increase in electron concentration over time, further improving the electrical conductivity. Under a longer laser irradiated time, the oxygen separation efficiency becomes gradually faster, resulting in more O_V. It is commonly accepted that weak or metastable chemical bonds (as hydrogen and OH species) widely exist within In_2O_3 film. The change of M-O lattices and O_V is caused by breaking the weak or metastable chemical bonds upon femtosecond laser irradiation, and the increase in laser irradiation time enhanced the breakdown process, leading to further removal of OH species and enhancement of O_V. Even though the In_2O_3 TFT fabricated by single thermal annealing process show higher percentage of O_V, the quantity of M-O lattices less than laser annealed TFTs caused by simplex low-temperature thermal annealing process. This is consistent with the XPS analysis of laser annealed In_2O_3 TFTs. And the FLA process can also promote conversion of the precursor to M-O lattices, leading to optimized arrangement of metal cations and oxygen anions to the lattice sites with an atomic-scale order, bolstered by photo-assisted densification reaction. Eventually a dense In_2O_3 film was formed. However, the longer the laser radiation time, the less the M-O lattices. After FLA process, the disparate change of M-O lattices and O_V indicate that the formation of M–O lattices and generation of O_V within In_2O_3 films were closely associated with laser radiation time. Simultaneously, the interface trap density also increases due to the mutual combination of H-bonding and constant growing O_V. The action that the interface trapped charge would suppress electron migration is expected to occur more frequently, indicating an increase in leakage current. After 30 s laser irradiation, the μ_{sat} values began to degrade significantly (from 10.03 ± 0.64 to 0.72 ± 0.03 cm^2/Vs), as shown in Table 1.

Generally, solution-processed In_2O_3 thin film required a thermal annealing process to convert metal-OH to M-O species. But the conversion of the precursor and the removal of impurity along with the formation of a dense film is much less than the laser annealed In_2O_3 films. The single low-temperature thermal annealing process increase the thermal budget and more inefficiently realize the dehydroxylation behavior for OH species, which hinder the mobility of charge. Meanwhile, a low amount of oxygen deficiency condition leads to the increase in O_V.Instead, the more effective conversion behavior from the FLA process improve the formation of M–O lattices and oxide frameworks. Efficient carrier transport in In_2O_3 TFTs could be achieved in oxide lattices more effectively than OH lattice, thus the FLA process lead to the improvement of charge transport. Overall, the proper ratio of M-O lattices and O_V is essential for improving the

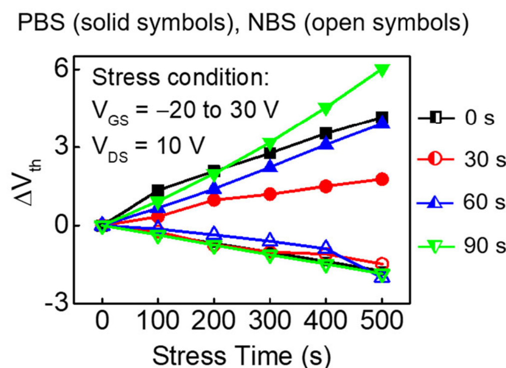

FIGURE 6. V_{TH} **shift as a function of the stress time. The time dependence of** ΔV_{TH} **in the** In_2O_3 **TFTs with various FLA times under** V_{GS} **from -20 to 30 V and** V_{GS} **of 10 V.**

electrical performance. Compared to single thermal annealing, the FLA-centered annealing technology at an optimal laser irradiation time of 30 s would improve the formation of M-O lattices more effectively, and higher mobility can be obtained.

Electrical stability under gate-bias-stress (GBS) is important for TFT devices. To gain further insight into the GBS of the In_2O_3 TFTs, the PBS (V_{GS} = 30 V) and NBS (V_{GS} = -20 V) were applied to the TFTs at V_{DS} = 10 V for 500 s. Figure 6 shows the threshold voltage shift (ΔV_{TH}) versus the stress time. The In_2O_3 TFTs fabricated by the FLA process at 30 s showed better stability of $\Delta V_{TH} \approx 1.5$ V under PBS and $\Delta V_{TH} \approx -1.5$ V under NBS conditions, with a negligible change in the SS value because additional traps were not produced during bias stressing [54] As the laser irradiation time increased, the In_2O_3 TFTs showed relatively stable NBS ($\Delta V_{TH} < 2$ V), but the ΔV_{TH} values on the PBS side also increased substantially. The TFTs fabricated at laser irradiation time of 90 s showed the most pronounced ΔV_{TH} of approximately 6 V. The long laser time irradiated TFTs resulted in instability due to the high trap density and a low carrier concentration in the interface between the electrode and the channel layer. These results, which can be explained by the interface trapping model, are partial and misleading. Nevertheless, the interaction between the channel layer and oxygen in an ambient atmosphere has an important influence on determining the instability [55], [56]. The channel layer stores abundant electrons during the GBS test in an ambient atmosphere, and the adsorption of oxygen molecules in the channel layer can deplete the electron carriers, leading to a positive shift of ΔV_{TH}, [57] as indicated in Figure 3(b-d). The change of ΔV_{TH} of laser annealed In_2O_3 TFTs with the persistent stress time means it is highly correlated with the defect creation and charge trapping inside the channel. Meanwhile, the generation of O_V was strongly associated with the laser irradiation time. The longer laser irradiation time, the higher the density of oxygen vacancies, leading to the instability due to the high trap density and a low carrier concentration in the interface between the electrode and the channel layer of the In_2O_3 films by 60 and 90 s FLA process [58], [59] In addition, the high interface trap density could disrupt the electrons flow and capture electrons. And then the change of trap density is reflected in the electrical transfer characteristic of TFT devices. An investigation of the laser irradiation time dependence of ΔV_{TH} showed that a short and optimal laser irradiation time is beneficial for the GBS stability, whereas an overlong time will degrade it.

The oxide TFTs device is generally affected by persistent positive and negative gate voltage stress, resulting in VTH shift and reduced service life. To characterize the effects of laser irradiation time on stability of In_2O_3 TFTs, the electrical bias stability was analyzed by PBS and NBS, but this test was done a few months later, so there will be a deviation in performance testing. Figure 7 shows the PBS and NBS results of single thermal annealed TFT and laser annealed TFT with various laser irradiation time when $V_{GS} = \pm 20$ V, $V_{DS} = 10$ V and stress duration of 500 s at room temperature. After stress of 500 s, the single thermal annealed In_2O_3 TFT exhibits an obvious positive ΔV_{TH} value of 2.5 V under the PBS state, meanwhile, the laser annealed TFTs both 60 and 90 s exhibit large and increased positive ΔV_{TH} of 6 and 8 V, as shown in Figure 7(a, c, d). However, the 30 s laser annealed In_2O_3 TFT showed an almost consistent ΔV_{TH} (< 1 V) under the identical PBS condition, fortunately, degradation mobility and SS values were not presented with the steady ΔV_{TH} compared with that of the other TFT devices. In the PBS test, the femtosecond laser caused the damage on the film surface during the FLA process, resulting in parallel positive ΔV_{TH} without the significant fluctuation in the SS value. Based on the above results, the improved PBS stability of 30 s laser annealed TFT is related with the increased O_V and interface trap density. This is also corresponded with above explains about the charge trapping and O_V defect at the channel and dielectric interface [59], [60] On the other hand, all the NBS stability tests of mentioned TFT device in this work were exhibited analogical ΔV_{TH} changes. And the ΔV_{TH} change under NBS with stress time of 500 s shows a smaller region of ΔV_{TH} (1.5 to 2 V), which is very similar with ΔV_{TH} (1.5 V) of 30 s laser annealed TFT under PBS condition, known from Figure 6. Combining the changes of ΔV_{TH} as a function of the stress time, it seems that NBS induce the activation of defects located deep in the activity layer, meanwhile, the defects lead to abnormal negative ΔV_{TH}. In general, heating pre-treatment and low-temperature annealing process can eliminate these defects [61] Therefore, the FLA process was applied to improve the NBS stability by removal of the defects and associated oxygen adsorption.

Figure 8 compares the time-dependent variations of the environmental stability of In_2O_3 TFTs, which were measured on the single low-temperature annealed device and devices fabricated with various laser irradiation times, for 1000 s. All the devices exhibited similar stability under the ambient environment to the 60 s sample device. An excessive laser irradiated time degrades the operational stability of the TFT device under the source-to-drain current. The device fabricated with the FLA process at 30 s provides optimal

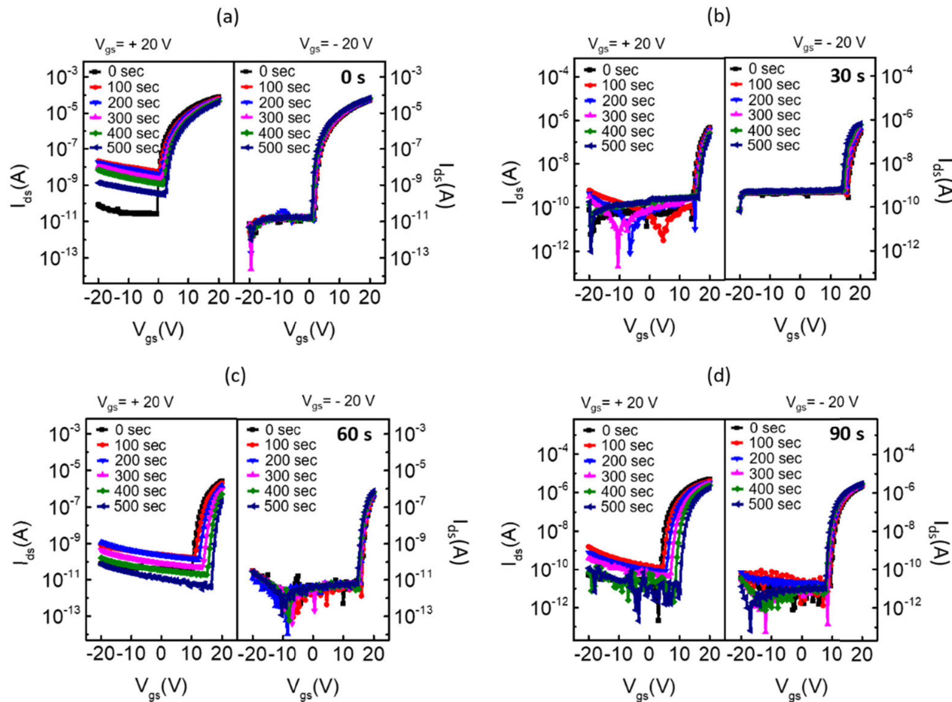

FIGURE 7. Evolution of the transfer curves as a function of PBS (left) and NBS (right) conditions for the (a) single thermal annealed In_2O_3 and FLA based In_2O_3 TFTs at laser irradiation time of (b) 30, (c) 60 and (d) 90 s. $V_{GS} = \pm 20$ V and $V_{DS} = 10$ V.

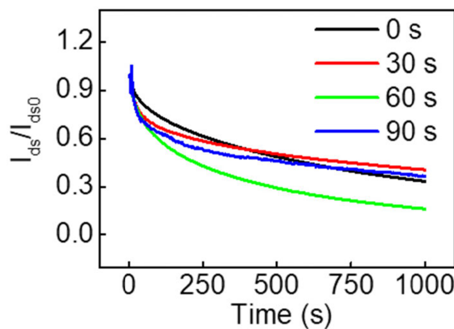

FIGURE 8. Time-dependent variation of the environmental stability of In_2O_3 TFTs with various FLA times.

operational stability. The process of the FLA at 30 s was superior to the additional laser irradiation time through a combination of the above analyses.

IV. CONCLUSION

The influence of FLA-centered low-temperature annealing processes for solution-processed In_2O_3 films, and the electrical performance of the TFT devices was investigated. The FLA-centered low-temperature preparation technology simplified the fabrication process and reduced energy consumption significantly. The electrical performance of In_2O_3 TFTs was enhanced significantly by applying the optimal laser irradiation time. The optimized preparation process combining the laser irradiation time at 30 s with a low annealing temperature of 230 °C, exhibited a high μ_{sat} of 10.03 ± 0.64 cm^2/Vs, an average I_{on}/I_{off} of 3.4×10^5, a low V_{TH} of 0.14 ± 0.64V, and a small SS of 1.44 ± 0.37 V/dec. These values were higher than those of a device fabricated using a thermal annealing process at 230 °C. In addition, In_2O_3 showed an extremely smooth surface with R_{RMS} less than 0.21 nm. The analysis indicated that the proper ratio of M-O lattices and O_V is essential for improving the electrical performance, and FLA-centered annealing technology at 30 s would improve the formation of M-O lattices more effectively. Furthermore, higher mobility and a negative shift in the V_{TH} was observed, indicating that the FLA-centered annealing technology at 30 s could optimize the V_{TH}, thereby reducing power consumption. Moreover, the influence of the laser irradiation time on the GBS test was investigated, showing better stability of ΔV_{TH} of 1.5 V under PBS and ΔV_{TH} of -1.5 V under NBS conditions through the FLA process at 30 s. Finally, the devices displayed similar stability under the ambient environment. This paper reports a novel annealing route for the fabrication of low-temperature solution-processed TFT devices. The results suggest the FLA-centered annealing technology may have applications in low-cost, low-power consumption, and large-area flexible electronics.

REFERENCES

[1] K. Nomura, H. Ohta, A. Takagi, T. Kamiya, M. Hirano, and H. Hosono, ''Room-temperature fabrication of transparent flexible thin-film transistors using amorphous oxide semiconductors,'' *Nature*, vol. 432, no. 7016, pp. 488–492, Nov. 2004.

[2] E. Fortunato, P. Barquinha, and R. Martins, ''Oxide semiconductor thin-film transistors: A review of recent advances,'' *Adv. Mater.*, vol. 24, no. 22, pp. 2945–2986, 2012.

[3] W. Xu, H. Li, J.-B. Xu, and L. Wang, "Recent advances of solution-processed metal oxide thin-film transistors," *ACS Appl. Mater. Interfaces*, vol. 10, no. 31, pp. 25878–25901, Aug. 2018.

[4] P. Weimer, "The TFT a new thin-film transistor," *Proc. IRE*, vol. 50, no. 6, pp. 1462–1469, Jun. 1962.

[5] C.-L. Lin, W.-Y. Chang, and C.-C. Hung, "Compensating pixel circuit driving AMOLED display with a-IGZO TFTs," *IEEE Electron Device Lett.*, vol. 34, no. 9, pp. 1166–1168, Sep. 2013.

[6] S.-H.-K. Park, C.-S. Hwang, M. Ryu, S. Yang, C. Byun, J. Shin, J.-I. Lee, K. Lee, M. S. Oh, and S. Im, "Transparent and photo-stable ZnO thin-film transistors to drive an active matrix organic-light- emitting-diode display panel," *Adv. Mater.*, vol. 21, no. 6, pp. 678–682, Feb. 2009.

[7] L. Petti, N. Münzenrieder, C. Vogt, H. Faber, L. Büthe, G. Cantarella, F. Bottacchi, T. D. Anthopoulos, and G. Tröster, "Metal oxide semiconductor thin-film transistors for flexible electronics," *Appl. Phys. Rev.*, vol. 3, no. 2, p. 021303, Jun. 2016.

[8] Y. Takeda, K. Hayasaka, R. Shiwaku, K. Yokosawa, T. Shiba, M. Mamada, D. Kumaki, K. Fukuda, and S. Tokito, "Fabrication of ultra-thin printed organic TFT CMOS logic circuits optimized for low-voltage wearable sensor applications," *Sci. Rep.*, vol. 6, no. 1, pp. 1–9, Sep. 2016.

[9] S. Jeong, Y.-G. Ha, J. Moon, A. Facchetti, and T. J. Marks, "Role of gallium doping in dramatically lowering amorphous-oxide processing temperatures for solution-derived indium zinc oxide thin-film transistors," *Adv. Mater.*, vol. 22, no. 12, pp. 1346–1350, Mar. 2010.

[10] P. K. Nayak, T. Busani, E. Elamurugu, P. Barquinha, R. Martins, Y. Hong, and E. Fortunato, "Zinc concentration dependence study of solution processed amorphous indium gallium zinc oxide thin film transistors using high-K dielectric," *Appl. Phys. Lett.*, vol. 97, no. 18, Nov. 2010, Art. no. 183504.

[11] Y.-H. Kim, J.-S. Heo, T.-H. Kim, S. Park, M.-H. Yoon, J. Kim, M. S. Oh, G.-R. Yi, Y.-Y. Noh, and S. K. Park, "Flexible metal-oxide devices made by room-temperature photochemical activation of sol–gel films," *Nature*, vol. 489, no. 7414, pp. 128–132, Sep. 2012.

[12] C.-G. Lee and A. Dodabalapur, "Solution-processed zinc–tin oxide thin-film transistors with low interfacial trap density and improved performance," *Appl. Phys. Lett.*, vol. 96, no. 24, Jun. 2010, Art. no. 243501.

[13] C. Avis and J. Jang, "High-performance solution processed oxide TFT with aluminum oxide gate dielectric fabricated by a sol-gel method," *J. Mater. Chem.*, vol. 21, no. 29, pp. 10649–10652, 2011.

[14] Y. S. Kim, W. J. Hwang, K. T. Eun, and S.-H. Choa, "Mechanical reliability of transparent conducting IZTO film electrodes for flexible panel displays," *Appl. Surf. Sci.*, vol. 257, no. 18, pp. 8134–8138, Jul. 2011.

[15] H. Nakazawa, Y. Ito, E. Matsumoto, K. Adachi, N. Aoki, and Y. Ochiai, "The electronic properties of amorphous and crystallized In_2O_3 films," *J. Appl. Phys.*, vol. 100, no. 9, Nov. 2006, Art. no. 093706.

[16] Y. G. Kim, T. Kim, C. Avis, S.-H. Lee, and J. Jang, "Stable and high-performance indium oxide thin-film transistor by ga doping," *IEEE Trans. Electron Devices*, vol. 63, no. 3, pp. 1078–1084, Mar. 2016.

[17] R. L. Weiher, "Electrical properties of single crystals of indium oxide," *J. Appl. Phys.*, vol. 33, no. 9, pp. 2834–2839, Sep. 1962.

[18] H. Kim, M. Osofsky, M. M. Miller, S. B. Qadri, R. C. Y. Auyeung, and A. Piqué, "Room temperature ferromagnetism in transparent fe-doped In_2O_3 films," *Appl. Phys. Lett.*, vol. 100, no. 3, Jan. 2012, Art. no. 032404.

[19] C. Y. Wang, V. Cimalla, H. Romanus, T. Kups, G. Ecke, T. Stauden, M. Ali, V. Lebedev, J. Pezoldt, and O. Ambacher, "Phase selective growth and properties of rhombohedral and cubic indium oxide," *Appl. Phys. Lett.*, vol. 89, no. 1, Jul. 2006, Art. no. 011904.

[20] Q. Liu, W. Lu, A. Ma, J. Tang, J. Lin, and J. Fang, "Study of quasi-monodisperse In_2O_3 nanocrystals: Synthesis and optical determination," *J. Amer. Chem. Soc.*, vol. 127, no. 15, pp. 5276–5277, 2005.

[21] A. Liu, G. X. Liu, H. H. Zhu, F. Xu, E. Fortunato, R. Martins, and F. K. Shan, "Fully solution-processed low-voltage aqueous In_2O_3 thin-film transistors using an ultrathin ZrO_x dielectric," *ACS Appl. Mater. Interfaces*, vol. 6, no. 20, pp. 17364–17369, 2014.

[22] D.-H. Lee, Y.-J. Chang, G. S. Herman, and C.-H. Chang, "A general route to printable high-mobility transparent amorphous oxide semiconductors," *Adv. Mater.*, vol. 19, no. 6, pp. 843–847, Mar. 2007.

[23] T. Kaneda, D. Hirose, T. Miyasako, P. T. Tue, Y. Murakami, S. Kohara, J. Li, T. Mitani, E. Tokumitsu, and T. Shimoda, "Rheology printing for metal-oxide patterns and devices," *J. Mater. Chem. C*, vol. 2, no. 1, pp. 40–49, 2014.

[24] S. Kaleemulla, A. S. Reddy, S. Uthanna, and P. S. Reddy, "Physical properties of In2O3 thin films prepared at various oxygen partial pressures," *J. Alloys Compounds*, vol. 479, nos. 1–2, pp. 589–593, Jun. 2009.

[25] J. H. Noh, S. Y. Ryu, S. J. Jo, C. S. Kim, S.-W. Sohn, P. D. Rack, D.-J. Kim, and H. K. Baik, "Indium oxide thin-film transistors fabricated by RF sputtering at room temperature," *IEEE Electron Device Lett.*, vol. 31, no. 6, pp. 567–569, Jun. 2010.

[26] S. Basharat, C. J. Carmalt, S. A. Barnett, D. A. Tocher, and H. O. Davies, "Aerosol assisted chemical vapor deposition of In_2O_3 films from Me3In and donor functionalized alcohols," *Inorganic Chem.*, vol. 46, no. 22, pp. 9473–9480, 2007.

[27] G. Shen, J. Xu, X. Wang, H. Huang, and D. Chen, "Growth of directly transferable In2O3 nanowire mats for transparent thin-film transistor applications," *Adv. Mater.*, vol. 23, no. 6, pp. 771–775, Feb. 2011.

[28] B. Zhu, X. Wu, W.-J. Liu, H.-L. Lu, D. W. Zhang, Z. Fan, and S.-J. Ding, "High-performance on-chip supercapacitors based on mesoporous silicon coated with ultrathin atomic layer-deposited In2O3 films," *ACS Appl. Mater. Interfaces*, vol. 11, no. 1, pp. 747–752, Jan. 2019.

[29] Z. Lin, L. Lan, S. Sun, Y. Li, W. Song, P. Gao, E. Song, P. Zhang, M. Li, L. Wang, and J. Peng, "Solution-processed high-mobility neodymium-substituted indium oxide thin-film transistors formed by facile patterning based on aqueous precursors," *Appl. Phys. Lett.*, vol. 110, no. 13, Mar. 2017, Art. no. 133502.

[30] J. Park, T. Gergely, Y. S. Rim, and S. Pyo, "Significant performance improvement of solution-processed metal oxide transistors by ligand dissociation through coupled temperature-time treatment of aqueous precursors," *ACS Appl. Electron. Mater.*, vol. 1, no. 4, pp. 505–512, 2019.

[31] Y. Hwan Hwang, J.-S. Seo, J. Moon Yun, H. Park, S. Yang, S.-H. K. Park, and B.-S. Bae, "An 'aqueous route' for the fabrication of low-temperature-processable oxide flexible transparent thin-film transistors on plastic substrates," *NPG Asia Mater.*, vol. 5, no. 4, p. e45, Apr. 2013.

[32] J. H. Park, Y. B. Yoo, K. H. Lee, W. S. Jang, J. Y. Oh, S. S. Chae, H. W. Lee, S. W. Han, and H. K. Baik, "Boron-doped peroxo-zirconium oxide dielectric for high-performance, low-temperature, solution-processed indium oxide thin-film transistor," *ACS Appl. Mater. Interfaces*, vol. 5, no. 16, pp. 8067–8075, Aug. 2013.

[33] T. Jun, K. Song, Y. Jeong, K. Woo, D. Kim, C. Bae, and J. Moon, "High-performance low-temperature solution-processable ZnO thin film transistors by microwave-assisted annealing," *J. Mater. Chem.*, vol. 21, no. 4, pp. 1102–1108, 2011.

[34] C. B. Jacobs, A. B. Maksov, E. S. Muckley, L. Collins, M. Mahjouri-Samani, A. Ievlev, C. M. Rouleau, J.-W. Moon, D. E. Graham, B. G. Sumpter, and I. N. Ivanov, "UV-activated ZnO films on a flexible substrate for room temperature O_2 and $H2_O$ sensing," *Sci. Rep.*, vol. 7, no. 1, pp. 1–10, Dec. 2017.

[35] S. B. Ameur, A. Barhoumi, H. Bel Hadjltaief, R. Mimouni, B. Duponchel, G. Leroy, M. Amlouk, and H. Guermazi, "Physical investigations on undoped and fluorine doped SnO_2 nanofilms on flexible substrate along with wettability and photocatalytic activity tests," *Mater. Sci. Semicond. Process.*, vol. 61, pp. 17–26, Apr. 2017.

[36] Q. Huang, W. Shen, X. Fang, G. Chen, Y. Yang, J. Huang, R. Tan, and W. Song, "Highly thermostable, flexible, transparent, and conductive films on polyimide substrate with an AZO/AgNW/AZO structure," *ACS Appl. Mater. Interfaces*, vol. 7, no. 7, pp. 4299–4305, Feb. 2015.

[37] K. K. Banger, Y. Yamashita, K. Mori, R. L. Peterson, T. Leedham, J. Rickard, and H. Sirringhaus, "Low-temperature, high-performance solution-processed metal oxide thin-film transistors formed by a 'sol–gel on chip' process," *Nature Mater.*, vol. 10, no. 1, pp. 45–50, Jan. 2011.

[38] S. Park, K. H. Kim, J. W. Jo, S. Sung, K. T. Kim, W. J. Lee, J. Kim, H. J. Kim, G. R. Yi, and Y. H. Kim, "In-depth studies on rapid photochemical activation of various sol-gel metal oxide films for flexible transparent electronics," *Adv. Funct. Mater.*, vol. 25, no. 19, pp. 2807–2815, 2015.

[39] M.-G. Kim, M. G. Kanatzidis, A. Facchetti, and T. J. Marks, "Low-temperature fabrication of high-performance metal oxide thin-film electronics via combustion processing," *Nature Mater.*, vol. 10, no. 5, pp. 382–388, May 2011.

[40] S. Son, T. S. Kim, J. S. Jung, M. K. Ryu, K. B. Park, B. W. Yoo, J. W. Kim, Y. G. Lee, J. Y. Kwon, and S. Y. Lee, "42.4 L: Late-news paper: 4 inch QVGA AMOLED driven by the threshold voltage controlled amorphous GIZO (Ga_2O_3-In_2O_3-ZnO) TFT," in *SID Symp. Dig. Tech. Papers*, vol. 39, no. 1, 2008, pp. 633–636.

[41] X. Li, J. Cheng, Y. Chen, Y. He, Y. Li, J. Xue, J. Guo, and Z. Yu, "Low-temperature aqueous route processed indium oxide thin-film transistors by NH_3 plasma-assisted treatment," *IEEE Trans. Electron Devices*, vol. 66, no. 3, pp. 1302–1307, Mar. 2019.

[42] C. Chen, G. Chen, H. Yang, G. Zhang, D. Hu, H. Chen, and T. Guo, "Solution-processed metal oxide arrays using femtosecond laser ablation and annealing for thin-film transistors," *J. Mater. Chem. C*, vol. 5, no. 36, pp. 9273–9280, 2017.

[43] R. R. Gattass and E. Mazur, "Femtosecond laser micromachining in transparent materials," *Nature Photon.*, vol. 2, no. 4, pp. 219–225, Apr. 2008.

[44] K. C. Phillips, H. H. Gandhi, E. Mazur, and S. K. Sundaram, "Ultrafast laser processing of materials: A review," *Adv. Opt. Photon.*, vol. 7, no. 4, pp. 684–712, 2015.

[45] G. Liu, A. Liu, H. Zhu, B. Shin, E. Fortunato, R. Martins, Y. Wang, and F. Shan, "Low-temperature, nontoxic water-induced metal-oxide thin films and their application in thin-film transistors," *Adv. Funct. Mater.*, vol. 25, no. 17, pp. 2564–2572, 2015.

[46] K. K. Banger, Y. Yamashita, K. Mori, R. L. Peterson, T. Leedham, J. Rickard, and H. Sirringhaus, "Low-temperature, high-performance solution-processed metal oxide thin-film transistors formed by a 'sol–gel on chip' process," *Nature Mater.*, vol. 10, no. 1, pp. 45–50, Jan. 2011.

[47] H. Wang, T. Sun, W. Xu, F. Xie, L. Ye, Y. Xiao, Y. Wang, J. Chen, and J. Xu, "Low-temperature facile solution-processed gate dielectric for combustion derived oxide thin film transistors," *RSC Adv.*, vol. 4, no. 97, pp. 54729–54739, 2014.

[48] S. Lee and D. C. Paine, "Identification of the native defect doping mechanism in amorphous indium zinc oxide thin films studied using ultra high pressure oxidation," *Appl. Phys. Lett.*, vol. 102, no. 5, Feb. 2013, Art. no. 052101.

[49] J. K. Jeong, J. H. Jeong, H. W. Yang, J.-S. Park, Y.-G. Mo, and H. D. Kim, "High performance thin film transistors with cosputtered amorphous indium gallium zinc oxide channel," *Appl. Phys. Lett.*, vol. 91, no. 11, Sep. 2007, Art. no. 113505.

[50] S.-H. Lee, T. Kim, J. Lee, C. Avis, and J. Jang, "Solution-processed gadolinium doped indium-oxide thin-film transistors with oxide passivation," *Appl. Phys. Lett.*, vol. 110, no. 12, Mar. 2017, Art. no. 122102.

[51] S. Y. Park, S. Kim, J. Yoo, K.-H. Lim, E. Lee, K. Kim, J. Kim, and Y. S. Kim, "Aqueous zinc ammine complex for solution-processed ZnO semiconductors in thin film transistors," *RSC Adv.*, vol. 4, no. 22, pp. 11295–11299, 2014.

[52] J. Socratous, K. K. Banger, Y. Vaynzof, A. Sadhanala, A. D. Brown, A. Sepe, U. Steiner, and H. Sirringhaus, "Electronic structure of low-temperature solution-processed amorphous metal oxide semiconductors for thin-film transistor applications," *Adv. Funct. Mater.*, vol. 25, no. 12, pp. 1873–1885, 2015.

[53] Y. S. Rim, H. S. Lim, and H. J. Kim, "Low-temperature metal-oxide thin-film transistors formed by directly photopatternable and combustible solution synthesis," *ACS Appl. Mater. Interfaces*, vol. 5, no. 9, pp. 3565–3571, May 2013.

[54] H. Y. Jung, Y. Kang, A. Y. Hwang, C. K. Lee, S. Han, D.-H. Kim, J.-U. Bae, W.-S. Shin, and J. K. Jeong, "Origin of the improved mobility and photo-bias stability in a double-channel metal oxide transistor," *Sci. Rep.*, vol. 4, no. 1, p. 3765, May 2015.

[55] J. K. Jeong, H. Won Yang, J. H. Jeong, Y.-G. Mo, and H. D. Kim, "Origin of threshold voltage instability in indium-gallium-zinc oxide thin film transistors," *Appl. Phys. Lett.*, vol. 93, no. 12, Sep. 2008, Art. no. 123508.

[56] T.-M. Pan, C.-H. Chen, J.-H. Liu, J.-L. Her, and K. Koyama, "Electrical and reliability characteristics of high-k $HoTiO_3$ a-InGaZnO thin-film transistors," *IEEE Electron Device Lett.*, vol. 35, no. 1, pp. 66–68, Jan. 2014.

[57] G. X. Liu, A. Liu, F. K. Shan, Y. Meng, B. C. Shin, E. Fortunato, and R. Martins, "High-performance fully amorphous bilayer metal-oxide thin film transistors using ultra-thin solution-processed ZrO_x dielectric," *Appl. Phys. Lett.*, vol. 105, no. 11, Sep. 2014, Art. no. 113509.

[58] A. Abliz, D. Wan, J.-Y. Chen, L. Xu, J. He, Y. Yang, H. Duan, C. Liu, C. Jiang, H. Chen, T. Guo, and L. Liao, "Enhanced reliability of In–Ga–ZnO thin-film transistors through design of dual passivation layers," *IEEE Trans. Electron Devices*, vol. 65, no. 7, pp. 2844–2849, Jul. 2018.

[59] A. Abliz, J. Wang, L. Xu, D. Wan, L. Liao, C. Ye, C. Liu, C. Jiang, H. Chen, and T. Guo, "Boost up the electrical performance of InGaZnO thin film transistors by inserting an ultrathin InGaZnO:H layer," *Appl. Phys. Lett.*, vol. 108, no. 21, May 2016, Art. no. 213501.

[60] H. E. Lee, S. Kim, J. Ko, H. I. Yeom, C. W. Byun, S. H. Lee, D. J. Joe, T. H. Im, S. H. K. Park, and K. J. J. A. F. M. Lee, "Skin-like oxide thin-film transistors for transparent displays," *Adv. Funct. Mater.*, vol. 26, no. 34, pp. 6170–6178, 2016.

[61] S. Jin, T.-W. Kim, Y.-G. Seol, M. Mativenga, and J. Jang, "Reduction of positive-bias-stress effects in bulk-accumulation amorphous-InGaZnO TFTs," *IEEE Electron Device Lett.*, vol. 35, no. 5, pp. 560–562, May 2014.

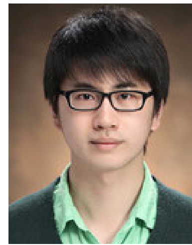

FEI SHAN received the M.S. and Ph.D. degrees in electrical and computer engineering from Chungbuk National University, Cheongju, South Korea, in 2017 and 2020, respectively. He is currently with the Research Institute for Computer and Information Communication, Chungbuk National University, as a Postdoctoral Research Fellow. His current research interests include the metal oxide devices, flexible printing electronics, large-area light sources, artificial intelligence hardware, and next generation memory devices.

HAO-ZHOU SUN received the B.S. degree from Chungbuk National University, Cheongju, South Korea, where he is currently pursuing the M.S. degree. His research interests include display thin film transistor and memory.

JAE-YUN LEE was born in Seoul, South Korea, in 1994. He is currently pursuing the joint B.S and M.S. degrees with the Graduate School, Chungbuk National University, South Korea. His current research interests include the fabrication of soluble oxide thin film transistors and next generation memory devices.

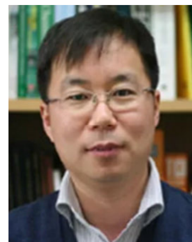

SEUNGMOON PYO received the Ph.D. degree in materials science and engineering from the University of California at Los Angeles, Los Angeles, in 2003. From 2003 to 2005, he worked with the Korea Research Institute of Chemical Technology (KRICT), Daejeon, South Korea, as a Senior Researcher. He is currently with the Department of Chemistry, Konkuk University, South Korea, as a Professor. His research interest includes the formation and analysis of organic electronic devices.

SUNG-JIN KIM received the B.S. and M.S. degrees from the Department of Electrical and Electronics Engineering, Kyungpook National University at Daegu, Daegu, South Korea, in 1999 and 2001, respectively, and the Ph.D. degree from the School of Electrical and Computer Engineering, Seoul National University, Seoul, South Korea, in 2006. From 2004 to 2007, he worked with Samsung SDI Company, the Cooperated Research and Development Center, Suwon, South Korea, as a Senior Research Engineer, where he developed various next-generation displays like flexible/bendable light sources and active matrix organic light-emitting diodes. In 2007, he was with the Department of Electrical Engineering, Columbia University, New York, NY, USA, as a Postdoctoral Research Scientist, where he was initially engaged in research on the application of organic thin-film transistors and new processing strategies for highly integrated organic systems. In 2008, he joined the School of Electrical and Computer Engineering, Georgia Institute of Technology, Atlanta, GA, USA, as a Postdoctoral Fellow, working on solution-processable organic light emitting diodes. In 2010, he was with the College of Electrical and Computer Engineering, Chungbuk National University, Cheongju, South Korea, as a Professor. His current research interests include the organic/oxide devices, flexible printing electronics, large-area light sources, and energy harvesting applications.